Pardeep K. Aggarwal,[1] Delma Veron,[1] David B. Thomas,[2] Dionicio Siegel,[3] Gilbert Moeckel,[4] Michael Kashgarian,[4] and Alda Tufro[1]

Semaphorin3a Promotes Advanced Diabetic Nephropathy

Diabetes 2015;64:1743–1759 | DOI: 10.2337/db14-0719

The onset of diabetic nephropathy (DN) is highlighted by glomerular filtration barrier abnormalities. Identifying pathogenic factors and targetable pathways driving DN is crucial to developing novel therapies and improving the disease outcome. Semaphorin3a (sema3a) is a guidance protein secreted by podocytes. Excess sema3a disrupts the glomerular filtration barrier. Here, using immunohistochemistry, we show increased podocyte SEMA3A in renal biopsies from patients with advanced DN. Using inducible, podocyte-specific *Sema3a* gain-of-function (*Sema3a*$^+$) mice made diabetic with streptozotocin, we demonstrate that sema3a is pathogenic in DN. Diabetic *Sema3a*$^+$ mice develop massive proteinuria, renal insufficiency, and extensive nodular glomerulosclerosis, mimicking advanced DN in humans. In diabetic mice, *Sema3a*$^+$ exacerbates laminin and collagen IV accumulation in Kimmelstiel-Wilson-like glomerular nodules and causes diffuse podocyte foot process effacement and F-actin collapse via nephrin, αvβ3 integrin, and MICAL1 interactions with plexinA_1. MICAL1 knockdown and sema3a inhibition render podocytes not susceptible to sema3a-induced shape changes, indicating that MICAL1 mediates sema3a-induced podocyte F-actin collapse. Moreover, sema3a binding inhibition or podocyte-specific *plexinA1* deletion markedly ameliorates albuminuria and abrogates renal insufficiency and the diabetic nodular glomerulosclerosis phenotype of diabetic *Sema3a*$^+$ mice. Collectively, these findings indicate that excess sema3a promotes severe diabetic nephropathy and identifies novel potential therapeutic targets for DN.

Diabetic nephropathy is the major cause of end-stage renal disease worldwide (1). It affects approximately 30% of both type 1 and type 2 diabetic patients. The precise determinants of susceptibility to developing diabetic nephropathy are unknown, and the pathogenic molecular mechanisms causing progression to renal failure are not fully understood (2,3). Thus identification of novel pathogenic factors and targetable signaling pathways mediating diabetic nephropathy is critical to developing new therapies and improving the disease outcome (4).

The onset of diabetic nephropathy is highlighted by glomerular filtration barrier functional and morphologic abnormalities, namely, microalbuminuria, hyperfiltration, glomerular basement membrane (GBM) thickening, and glomerulomegaly (2,5). Vascular endothelial growth factor (VEGF)-A locally mediates some of these changes, modulated by reactive oxygen species, advanced glycosylation end products, angiotensin II, and low nitric oxide, which act in concert with the diabetic milieu (reviewed by Forbes and Cooper [2] and Tufro and Veron [6]). Additional angiogenic factors, such as platelet-derived growth factor-B and angiopoietin 2, contribute to the development of proteinuria in diabetic mice (7–11).

Semaphorin3a (sema3a), a member of the Semaphorin family of guidance proteins, is characterized by the ability to collapse the actin cytoskeleton and disassemble F-actin in multiple cell types (12,13). Podocytes and ureteric bud-derived tubular cells synthesize sema3a in the kidney (14). *Sema3a* is required for normal development of the glomerular filtration barrier and podocyte differentiation (15), but *Sema3a* gain of function disrupts the slit diaphragm, causing foot process effacement and proteinuria (15,16). Sema3a cell autonomously induces podocyte contraction and F-actin collapse (16). A membrane protein complex consisting of a binding receptor, neuropilin1, and a signaling receptor,

[1]Department of Pediatrics/Nephrology, Yale University School of Medicine, New Haven, CT
[2]Department of Pathology, University of Miami Miller School of Medicine, Miami, FL
[3]Skaggs School of Pharmacy and Pharmaceutical Sciences, University of California, San Diego, La Jolla, CA
[4]Department of Pathology, Yale University School of Medicine, New Haven, CT
Corresponding author: Alda Tufro, alda.tufro@yale.edu.

Received 5 May 2014 and accepted 26 November 2014.
This article contains Supplementary Data online at http://diabetes.diabetesjournals.org/lookup/suppl/doi:10.2337/db14-0719/-/DC1.

plexinA_1, mediates sema3a signals (12,17,18). Neuropilin1 is also a coreceptor for VEGF-A, and both ligands, sema3a and VEGF-A, compete for neuropilin1 binding (19). PlexinA_1 intracellular signaling involves several pathways to regulate cell shape and cytoskeleton, including integrins, molecules interacting with CasL (MICALs), collapsing response mediator protein, and small GTPases, as well as interactions with receptor tyrosine kinases and other membrane proteins (reviewed by Tran et al. [12]). In podocytes, plexinA_1 interacts directly with nephrin (16). MICALs are cytoplasmic flavin mono-oxygenases that regulate cell shape, migration, and exocytosis through a redox-dependent mechanism (20). MICALs directly bind plexinA receptors and induce F-actin loss by decreasing actin polymerization, bundling, and branching (21–23), thereby linking extracellular semaphorin signals to actin dynamics and the cytoskeleton (13,21).

We observed sema3a upregulation in diabetic mouse kidneys (24), but the pathophysiologic function of sema3a in diabetic nephropathy remains unknown. To determine whether this finding is relevant for human diabetic nephropathy, we examined renal biopsies from diabetic patients. Here we report that sema3a is upregulated in human diabetic nephropathy. Using a diabetic, inducible gain-of-function mouse model, we provide evidence that sema3a is pathogenic in diabetic nephropathy, promoting advanced diabetic nodular glomerulosclerosis and leading to massive proteinuria and renal failure. We found that, in the context of diabetes, sema3a causes diffuse podocyte foot process effacement and F-actin collapse via nephrin, αvβ3 integrin, and MICAL1 interactions with plexinA_1. MICAL1 knockdown or sema3a binding inhibition abrogates sema3a-induced F-actin collapse in podocytes. Moreover, sema3a inhibition in vivo or podocyte-specific *plexinA1* deletion significantly attenuates diabetic nephropathy. Collectively, these data reveal that excess sema3a promotes severe diabetic nephropathy and identify novel potential therapeutic targets for diabetic nephropathy.

RESEARCH DESIGN AND METHODS

Human Kidney Biopsy Studies

Frozen sections of de-identified kidney biopsy samples from human patients diagnosed with class III or IV diabetic nephropathy (n = 6; 1 with type 1 diabetes, 2 with type 2 diabetes, 3 with unspecified diabetes mellitus) or nondiabetic renal disease (n = 4; 1 with hypertension, 1 with obesity, 2 with proteinuria) were obtained from NephroCor following institutional review board approval of the study. Sema3a and podocin fluorescent immunohistochemistry were performed as described elsewhere (24).

Animal Studies

In *podocin-rtTA:tet-O-Sema3a* mice generated previously (15) (herein called *Sema3a*$^+$ mice), an FVB genetic background was maintained for >10 generations. Diabetes was induced (low-dose Animal Models of Diabetic Complications Consortium [AMDCC] protocol) in 6- to 8-week-old male *Sema3a*$^+$ mice by intraperitoneal administration of streptozotocin (STZ; 50 mg/kg) five times daily (24). Diabetes (random blood glucose concentration >300 mg/dL) was confirmed using a glucose oxidase biosensor blood glucose meter (OneTouch Ultra-2; LifeScan) 1 week after the last STZ injection. Diabetic *Sema3a*$^+$ (DM-*Sema3a*$^+$; n = 15) and non-DM-*Sema3a*$^+$ mice (n = 18) were fed a diet containing doxycycline (0.625 mg/kg chow; Harlan-Teklad) or standard chow for 12–16 weeks. After 12–16 weeks of diabetes, 24 h of urine was collected in metabolic cages; blood and kidney samples were collected under anesthesia. For sema3a inhibition studies, DM-*Sema3a*$^+$ mice were fed chow containing doxycycline for 8 weeks, then Alzet osmotic pumps (Model 1004) containing xanthofulvin (0.5 mg/mL in PBS; n = 4) (25) or saline (n = 2) were implanted subcutaneously. All mice were fed doxycycline-containing chow for the following 4 weeks.

Generation of Conditional Podocyte-Specific PlexinA_1 Knockout Mice

To selectively delete *plexinA1* in podocytes in a doxycycline-dependent manner, previously reported *plexinA1*$^{+/fl}$ mice (26) were bred with *tet-Cre* mice (27) and double heterozygous mice were bred to *Sema3a*$^+$ mice, maintaining an FVB background. Quadruple transgenic mice (*plexinA1*$^{fl/fl}$*:tet-O-Cre:podocin-rtTA:tet-O-Sema3a*; n = 6) and their double or triple transgenic littermates lacking the tet-regulated transgenes were made diabetic (n = 5), fed a diet containing doxycycline, and examined after 12 weeks, following the protocol described above. Genotyping was performed by PCR using previously reported primers (15,26,27). All animal protocols were approved by the Yale Animal Care and Use Committee.

Renal Phenotype Analysis

Urinary albumin was measured using mouse albumin ELISA (Bethyl Laboratories) and SDS-PAGE/Coomassie blue staining, as described elsewhere (16). Plasma and 24-h urine creatinine were measured by high-performance liquid chromatography (16). Transmission electron microscopy (TEM) was performed using standard techniques (16). Glomerular area was measured using ImageJ software (National Institutes of Health, Bethesda, MD; http://rsb.info.nih.gov/ij/) in 34 ± 2.1 glomeruli/kidney from 4 mice per experimental condition. A renal pathologist (G.M.) examined in a blinded fashion kidney specimens stained with periodic acid Schiff and assigned a semiquantitative pathology score based on the percentage of the area (0 = none; 1 = 1–25%; 2 = 26–50%; 3 = 51–75%; 4 = 76–100%) with the following features: glomerular nodules, mesangiolysis, mesangial sclerosis, and interstitial fibrosis (24). The percentage of glomeruli per section containing mesangiolysis or nodules was calculated (28).

Mouse Plasma and Urine Sema3a ELISA

Plasma and urine samples, appropriately diluted, were dispensed into microtiter plates and incubated overnight

at 4°C. Plates were washed, blocked with 5% powdered milk in wash buffer, and incubated with sema3a antibody (sc-1148; Santa Cruz Biotechnology) for 2 h at 37°C, followed by extensive washes. Plates then were incubated in peroxidase-conjugated rabbit antigoat IgG (305–035–003; Jackson ImmunoResearch Laboratories) for 1 h at 37°C and washed, followed by incubation in peroxidase substrate (34022; Pierce) for 30 min, 2 mol/L H_2SO_4. Optical density was measured at 450 nm using a microplate reader (BioRad). Recombinant mouse sema3a (15) served as the standard.

Immunohistochemistry

Fluorescent immunostaining studies were performed on frozen kidney sections, as described elsewhere (15), using the following primary antibodies: antilaminin (L9393; Sigma), collagen IV (Southern Biotech), sema3a (R&D AF1250), nephrin (20R-NP002; Fitzgerald Inc.), WT1 (sc-192; Santa Cruz), podocin (P0372; Sigma), and αvβ3 integrin (EMD Millipore). Dual immunolabeling was performed using appropriate Cy2 and Cy3 fluorescent-tagged secondary antibodies (Jackson ImmunoResearch Laboratories), and signals were visualized by confocal microscopy (FluoView 300; Olympus) and quantitated using ImageJ software (16).

Immunoblot Analysis

Equal amounts of protein from four or more kidney lysates per experimental condition were pooled and resolved by SDS-PAGE. Using a standard technique, immunoblotting was performed with the following primary antibodies: WT1, podocin, nephrin, laminin, sema3a (sc-28867; Santa Cruz), β3-integrin (sc-14009; Santa Cruz), β1-integrin (AB1952; EMD Millipore), neuropilin1 (17), matrix metalloproteinase (MMP)-2 (MAB13434; EMD Millipore), MMP-9 (AB19016; EMD Millipore), plexinA_1 (sc-25639; Santa Cruz), VEGF receptor 2 (2479; Cell Signaling Technologies), and MICAL1 (14818–1-AP; Proteintech). Actin (A2066; Sigma) or tubulin (Sigma) was used as a loading control. Signals were detected with appropriate horseradish peroxidase–conjugated secondary antibodies, visualized by chemiluminescence, and quantified using ImageJ software.

PlexinA_1-MICAL1 Coimmunoprecipitation

Sema3a$^+$ podocytes were lysed in immunoprecipitation buffer, as described elsewhere (16). Lysates were precleared, incubated with MICAL1 antibody (14818–1-AP; Proteintech), incubated overnight with protein A agarose, eluted, and analyzed by immunoblotting using plexinA_1, MICAL1, and actin antibodies, detected by enhanced chemiluminescence. Rabbit serum served as the negative control, and lysate from MICAL1/plexinA_1-transfected HEK cells served as the positive control.

Podocyte Morphology Assay

Sema3a$^+$ podocyte cell line was described previously (16). *Sema3a*$^+$podocytes were exposed to RPMI 1640 medium plus 1% FBS, RPMI 1640 medium plus 0.1 μmol/L xanthofulvin, RPMI 1640 medium plus 100 ng/mL rat recombinant sema3a (15), or RPMI 1640 medium plus xanthofulvin and sema3a for 16 h and then were fixed and stained with rhodamine-phalloidin (16). Images were acquired (Zeiss Axiovert) and the podocyte area (square micrometers) was measured using Zeiss AxioVision software, as described previously (16); 71 ± 4 cells per experimental condition from three independent experiments were measured.

Podocyte MICAL1 Knockdown and Morphology Assay

Podocyte MICAL1 knockdown was induced using a mouse MICAL1 small interfering RNA (siRNA) oligonucleotide (CAGGUGCCAUGACUAAGUAUU) (Dharmacon) (29). Briefly, podocytes were transfected with 200 pmol MICAL1 siRNA or scrambled siRNA using Oligofectamine (Invitrogen) and incubated for 72 h. MICAL1 knockdown was confirmed by immunoblot. Podocytes with or without MICAL1 knockdown were exposed for 6 h to mouse recombinant sema3a (100 ng/mL). Podocytes were fixed, permeabilized, and stained with rhodamine-phalloidin; their morphology was analyzed as described above.

Statistical Analysis

Data are expressed as mean ± SEM. Unpaired Student *t* test or ANOVA were used to compare experimental groups, as appropriate. Linear association between two variables was evaluated by Pearson correlation, and association between categorical variables was assessed using the Fischer exact test. $P < 0.05$ was deemed statistically significant.

RESULTS

Podocyte SEMA3A Is Increased in Human Diabetic Nephropathy

Dual immunostaining of renal biopsy sections from type 1 and type 2 diabetic patients with class III and IV diabetic nephropathy (n = 6) with sema3a and podocin antibodies revealed significantly more immunoreactive SEMA3A localized to podocytes (Fig. 1*A–C* and *H*) than in nondiabetic patients (n = 4) with hypertension, obesity, or proteinuria due to minimal change disease (MCD) (Fig. 1*D–G*). Immunoreactive SEMA3A also was detected in renal tubules in all biopsies examined but was not differentially expressed in diabetic and nondiabetic specimens. Quantitation of immunofluorescent signals showed almost twofold higher glomerular SEMA3A in diabetic than in nondiabetic glomeruli (Fig. 1*I* and *J*).

Sema3a$^+$ Gain of Function Increases Plasma and Urine sema3a in Diabetic Mice

To determine whether excess podocyte sema3a influences the severity of diabetic nephropathy, we used an inducible podocyte *Sema3a*$^+$ gain-of-function mouse model, made diabetic by low-dose streptozotocin (AMDCC protocol) (24), that increases renal sema3a two- to fourfold (15). Genetically identical diabetic and nondiabetic mice were fed

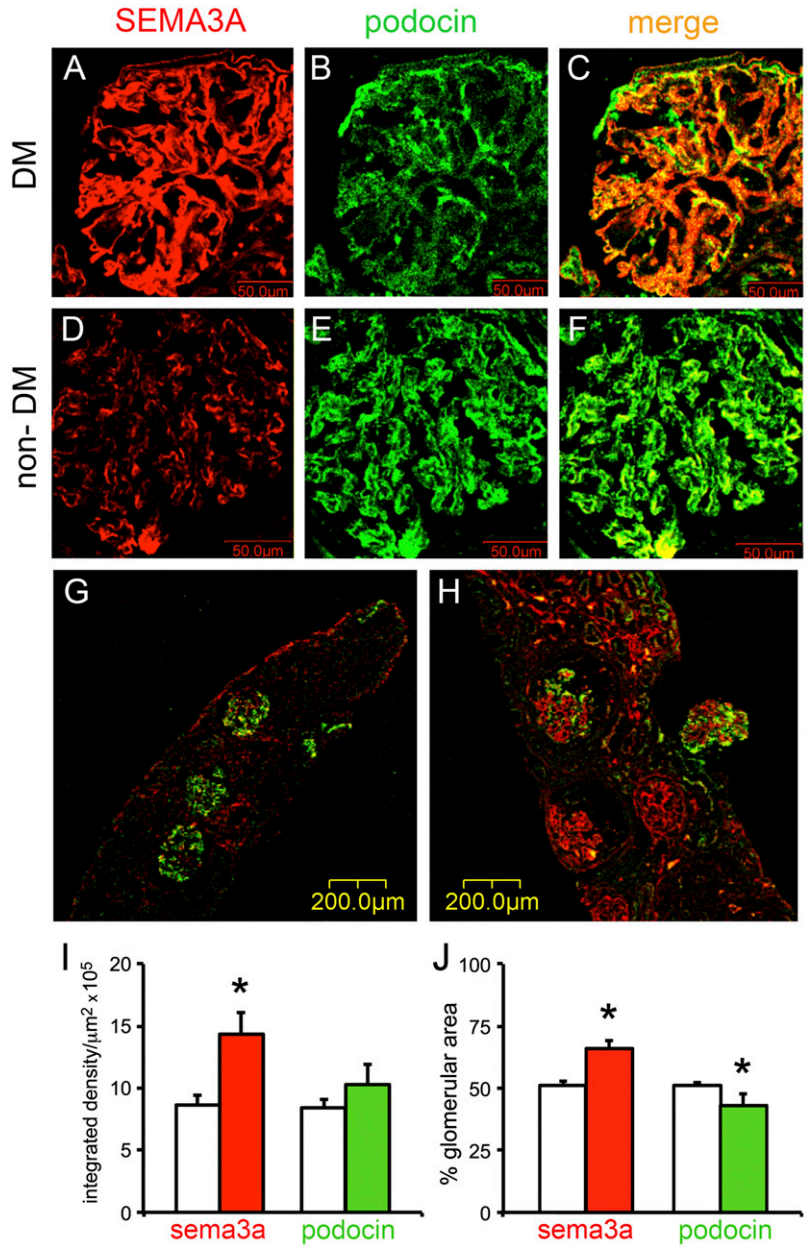

Figure 1—Podocyte SEMA3A is increased in human diabetic nephropathy. Dual fluorescent immunohistochemistry with SEMA3A and NPH2 antibodies was performed in frozen sections from human renal biopsies. *A–C*: Representative images from a biopsy with class IV diabetic nephropathy show a strong SEMA3A signal (*A*, red) localized to podocytes, as indicated by colocalization with podocin (*B*, green) shown in a merge (*C*, yellow/orange). Scale bars = 50 μm. *D–F*: Representative images from a nondiabetic kidney biopsy (a patient with hypertension and no evidence of renal pathology) show minimal SEMA3A signal localized to podocytes. Scale bars = 50 μm. *G*: Representative low-magnification image from nondiabetic kidney biopsy (MCD) shows minimal SEMA3A in three glomeruli, whereas podocin expression is intact. Scale bar = 200 μm. *H*: Representative low-magnification image from a diabetic kidney biopsy shows strong glomerular SEMA3A expression and variable colocalized podocin expression. Scale bar = 200 μm. *I* and *J*: Quantitation of immunofluorescent signals shows that SEMA3A increases approximately twofold in diabetic glomeruli (red bars) compared with nondiabetic glomeruli (white bars), whereas podocin (green bars) does not change or decreases slightly. Data are expressed as mean ± SEM immunofluorescent integrated density/μm^2 (*I*) and percentage of glomerular area stained on immunofluorescence (*J*). All glomeruli present in the biopsies were included in this quantitative analysis. DM, diabetes mellitus.

doxycycline-containing or standard chow for 12–16 weeks (15). Plasma sema3a concentrations were similar in control diabetic and nondiabetic mice (Fig. 2*A*), suggesting that the diabetic milieu per se does not increase sema3a. By contrast, podocyte *Sema3a*$^+$ gain of function increased sema3a plasma concentrations in both nondiabetic and diabetic mice (Fig. 2*A*), suggesting that podocyte sema3a secretion is a significant determinant of sema3a plasma concentrations. The increase in Sema3a was larger (approximately threefold vs. twofold) in diabetic mice than in nondiabetic

mice, likely because of changes in clearance. Podocyte *Sema3a*$^+$ gain of function increased sema3a excretion approximately eightfold and urine output increased approximately fourfold in diabetic mice, whereas no change in sema3a excretion was detected in nondiabetic mice (Fig. 2*B* and *J*), suggesting that diabetes exacerbates sema3a secretion. Glomerular immunoreactive sema3a was increased in *Sema3a*$^+$ diabetic mice (Supplementary Fig. 1), as previously described in mice with advanced diabetic glomerulosclerosis (24).

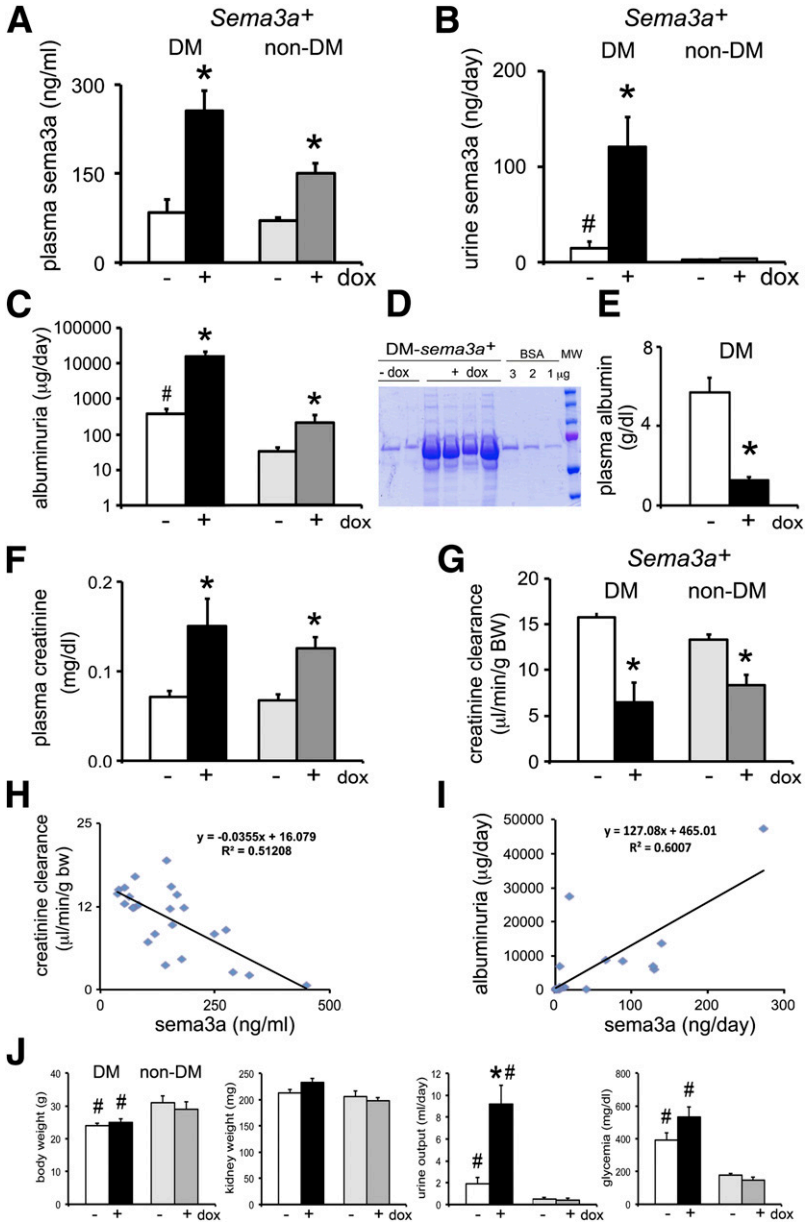

Figure 2—Excess Sema3a in diabetic mice causes massive proteinuria and renal failure. *A*: *Sema3a*$^+$ gain of function and diabetes have additive effects, increasing plasma concentrations of sema3a. *B*: Diabetes increases sema3a excretion, and *Sema3a*$^+$ gain of function induces a synergistic increase. *C*: Quantification of albuminuria by ELISA (notice the logarithmic scale): *Sema3a*$^+$ gain of function in diabetic mice causes massive albuminuria, ~40-fold higher than in control diabetic mice. *D*: Coomassie blue stain of urine resolved by SDS-PAGE illustrates proteinuria (in the nephrotic range) in diabetic mice with *Sema3a*$^+$ gain of function (DM-*Sema3a*$^+$ +dox). *E*: Diabetic mice with *Sema3a*$^+$ gain of function develop hypoalbuminemia. *F–H*: *Sema3a*$^+$ gain of function in diabetic mice induces renal failure. *F*: *Sema3a*$^+$ gain of function induces a doubling of plasma creatinine in diabetic mice and a lesser increase in nondiabetic mice. Creatinine clearance decreases ~60% in diabetic mice with *Sema3a*$^+$ gain of function (*G*) and correlates inversely with plasma sema3a concentration (*H*). *I*: Albuminuria correlates directly with urine sema3a excretion. *J*: Bar graphs show body weight, kidney weight, urine output, and blood glucose in all experimental groups. Notice severe polyuria in *Sema3a*$^+$ gain-of-function diabetic compared with control diabetic mice, without a significant change in random blood glucose. *$P < 0.05$ vs. corresponding control. #$P < 0.05$ vs. nondiabetic control. White bars are diabetic controls (-dox); black bars are diabetic sema3a gain-of-function (+dox); light gray are nondiabetic (-dox); dark gray are nondiabetic sema3a gain-of-function (+dox). BW, body weight; DM, diabetes mellitus; dox, doxycycline; MW, molecular weight.

Sema3a$^+$ Gain of Function in Diabetic Mice Causes Massive Proteinuria and Renal Failure

Induction of podocyte *Sema3a*$^+$ gain of function in diabetic mice dramatically exacerbates albuminuria to ~40-fold higher than diabetic controls (Fig. 2*C* and *D*; note the logarithmic scale in 2*C*). This massive proteinuria results in nephrotic syndrome, indicated by associated hypoalbuminemia (Fig. 2*E*). By contrast, nondiabetic *Sema3a*$^+$gain-of-function mice develop modest albuminuria (Fig. 2*C*), and their plasma albumin remains normal (4.8 ± 0.65 g/dL). Podocyte *Sema3a*$^+$ gain of function in diabetic mice decreases creatinine clearance by ~60% and increases plasma creatinine more than twofold (Fig. 2*F* and *G*), whereas creatinine clearance decreases ~35% in nondiabetic mice. Creatinine clearance correlates inversely with plasma sema3a (Fig. 2*H*), and albuminuria correlates directly with sema3a urine excretion (Fig. 2*I*). General parameters are shown in Fig. 2*J*.

Sema3a$^+$ Gain of Function in Diabetic Mice Causes Advanced Diabetic Nephropathy

Examination of uninduced nondiabetic kidneys showed normal histology (Fig. 3*A*), whereas induction of *Sema3a*$^+$gain of function resulted in mesangial expansion (Fig. 3*B*), as previously described (16). Uninduced diabetic kidneys (DM-*Sema3a*$^+$–dox) showed mesangial expansion and glomerulomegaly, the expected mild STZ-induced diabetic nephropathy phenotype (Fig. 3*C* and *D*). By contrast, diabetic kidneys with *Sema3a*$^+$ gain of function (DM-*Sema3a*$^+$+dox) with an identical genotype revealed extensive mesangiolysis, nodular and diffuse glomerulosclerosis, as well as mesangial sclerosis, arteriolar hyalinosis, interstitial fibrosis, protein casts, and fibrin caps, consistent with advanced diabetic nephropathy (Fig. 3*E*–*M*). Blinded morphometric analysis confirmed these observations, summarized by a semiquantitative pathological score including glomerular nodules, mesangiolysis, mesangial sclerosis, and interstitial fibrosis (Fig. 3*N*). Quantitation of Kimmelstiel-Wilson-like nodules showed that 55 ± 4% of glomeruli from diabetic *Sema3a*$^+$ gain-of-function mice have periodic acid Schiff–positive nodules, whereas no nodules were observed in glomeruli from control diabetic mice (0 ± 0%) (Fig. 3*N*). The nonrandom association of *Sema3a*$^+$gain of function with glomerular nodules and mesangiolysis in diabetic mice was confirmed by Fischer exact tests ($P = 0.0079$ and $P = 0.047$, respectively). Together, these findings demonstrate that *Sema3a*$^+$ gain of function induces diabetic nodular glomerulosclerosis and advanced diabetic nephropathy.

TEM of diabetic control kidneys showed mild, focal foot process effacement and GBM thickening (Fig. 4*A*). By contrast, diabetic kidneys with *Sema3a*$^+$ gain of function revealed diffuse foot process effacement, podocyte vacuoles, absence of slit diaphragms, GBM thickening (Fig. 4*B*), and endothelial injury consisting of glomerular endothelial cell swelling, detachment with expansion of the subendothelial space and narrowing of the capillary lumen, as well as extensive mesangial sclerosis and fibrillar electron-dense deposits in some nodules (Fig. 4*E*). No microthrombi or fibrin deposition was observed. Uninduced nondiabetic *Sema3a*$^+$mice had a normal glomerular ultrastructure (Fig. 4*C*). In nondiabetic mice, *Sema3a*$^+$ gain of function induced significantly less severe podocyte and endothelial cell lesions (Fig. 4*D*), as previously described (16). Quantitation of ultrastructural abnormalities showed that all diabetic kidneys had a significantly thicker GBM than nondiabetic ones; *Sema3a*$^+$ gain of function caused further GBM thickening and a more than threefold increase of podocyte foot process width in diabetic mice compared with diabetic and nondiabetic controls (Fig. 4*F* and *G*). Collectively, TEM findings indicate that *Sema3a*$^+$ gain of function in diabetic mice exacerbates the hallmark features of diabetic nephropathy, leading to class IV–like diabetic nodular glomerulosclerosis.

Laminin and Collagen IV Are Increased in DM-Sema3a$^+$ Glomerular Nodules

Laminin and collagen IV were significantly increased in glomeruli of *Sema3a*$^+$ gain-of-function diabetic mice (Fig. 5*A*–*C*), although total kidney laminin was decreased (Fig. 5*D*). Expression of MMP-2 and -9, major glomerular collagenases, was downregulated in *Sema3a*$^+$ gain-of-function mice (Fig. 5*E*), consistent with the collagen IV accumulation observed by immunohistochemistry. Since podocyte *VEGF-A* gain of function in diabetic mice causes nodular glomerulosclerosis (24), we examined VEGF-A expression in *Sema3a*$^+$ diabetic mice. Plasma concentrations of VEGF-A were higher in all diabetic mice (irrespective of transgene induction) than in nondiabetic mice, but kidney VEGF-A and VEGFR2 expression were downregulated in *Sema3a*$^+$ gain-of-function diabetic mice (Fig. 5*F*–*H*), indicating that excess VEGF-A is not a determinant of glomerular nodule development in diabetic *Sema3a*$^+$ gain-of-function mice.

Sema3a$^+$ Gain of Function Downregulates Nephrin, WT-1, and αvβ3 Integrin and Accentuates Podocytopenia in Diabetic Mice

Nephrin was downregulated in all diabetic mice (Fig. 6*A*, *B*, and *E*). Podocin was not significantly decreased by immunoblotting or immunofluorescence (Fig. 6*B* and *E*), except in extensively damaged glomeruli (Fig. 6*D*). In addition, *Sema3a*$^+$ gain of function induced a marked downregulation of WT1 that was not observed in control diabetic mice (Fig. 6*B*). Exacerbation of podocytopenia was confirmed by WT1$^+$ cell count (Fig. 6*C*). *Sema3a*$^+$ gain of function induced αvβ3 integrin downregulation in diabetic glomeruli (Fig. 6*D* and *E*), suggesting that decreased integrin activity may contribute to podocyte loss. Increased podocytopenia is consistent with the observation of focal GBM denudation in glomeruli of *Sema3a*$^+$ gain-of-function diabetic mice (Fig. 6*H*).

MICAL1 Mediates Sema3a-Induced Podocyte F-Actin Collapse

We examined sema3a signaling in the kidney downstream from plexinA_1–nephrin interaction (16). Immunoblotting

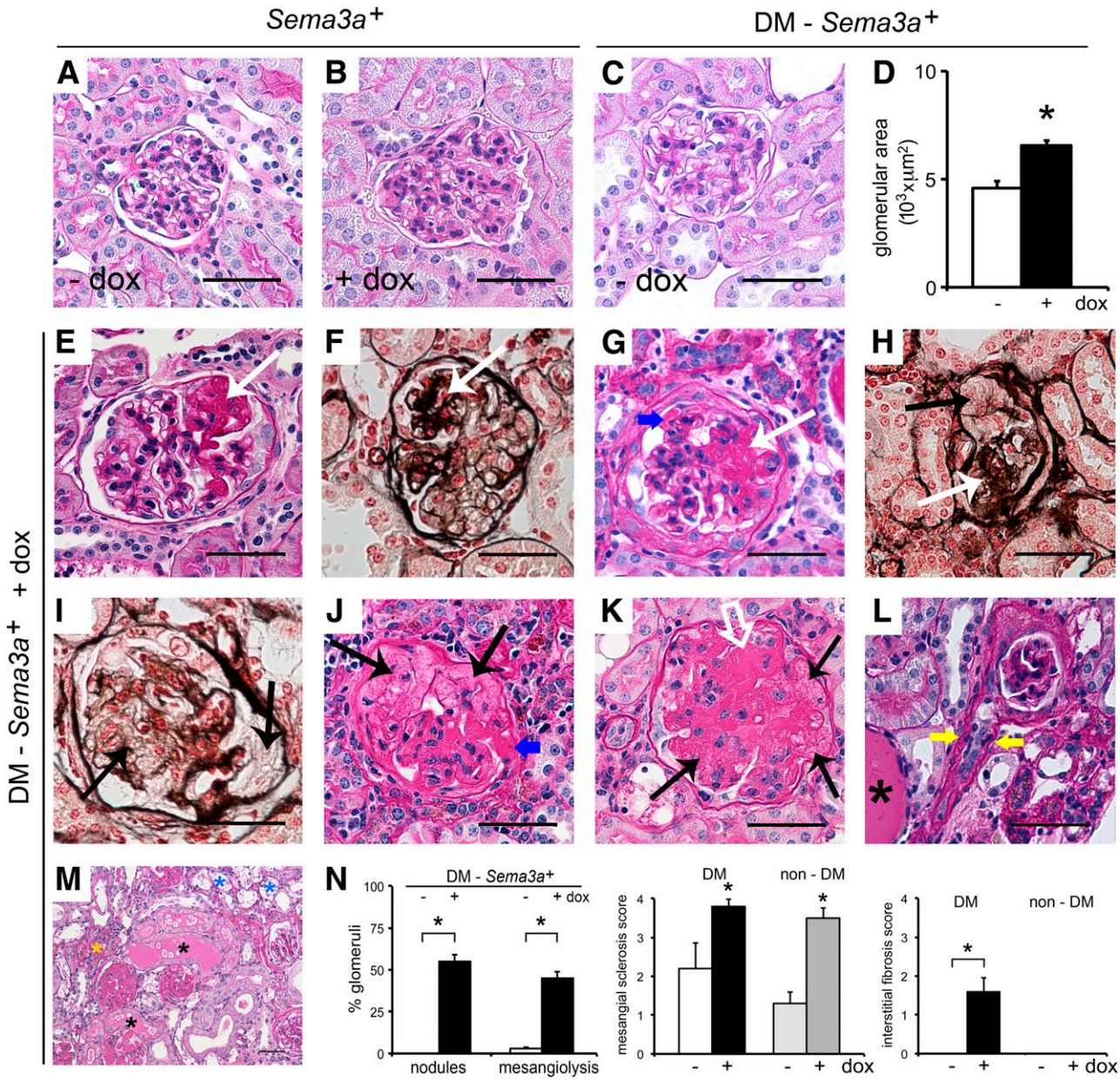

Figure 3—*Sema3a*$^+$ gain of function in diabetic mice causes advanced diabetic nephropathy. Periodic acid Schiff (PAS) stain of non-diabetic kidneys (*Sema3a*$^+$) shows normal histology in control kidney (-dox) (*A*), whereas a kidney from a mouse receiving doxycycline (+dox) shows mesangial expansion (*B*). *C:* PAS staining of a biopsy sample from a control diabetic kidney (diabetes mellitus [DM]-*Sema3a*$^+$ -dox) shows mild mesangial expansion. *D*: Quantification of glomerular area indicates that *Sema3a*$^+$ gain of function in diabetic mice induces glomerulomegaly (DM-*Sema3a*$^+$ +dox vs. DM-*Sema3a*$^+$ -dox; n = 4 kidneys each, 34 ± 2 glomeruli/kidney). *E–M*: PAS and Jones' silver stains of *Sema3a*$^+$ gain-of-function diabetic kidneys (DM-*Sema3a*$^+$ +dox) show nodular Kimmelstiel-Wilson-like glomerulosclerosis (white arrows), mesangiolysis (black arrows), diffuse glomerulosclerosis (white open arrow), fibrin caps (blue arrows), arteriolar hyalinosis (yellow arrows), foam cells (blue asterisks), protein casts (black asterisks), and interstitial infiltrates (yellow asterisk). *N*: Quantification of glomerular nodules and mesangiolysis, shown as a percentage of glomeruli with nodules or mesangiolysis per kidney in diabetic *Sema3a*$^+$ gain-of-function (+dox) vs. diabetic control mice (-dox) (134 ± 6 and 121 ± 5 glomeruli/kidney were counted in n = 5 and n = 4 kidneys, respectively; $P < 0.05$). Semiquantitative pathology score shows significantly increased mesangial sclerosis in all *Sema3a*$^+$ gain-of-function kidneys, whereas interstitial fibrosis occurs exclusively in *Sema3a*$^+$ gain-of-function diabetic mice (black bars). Scale bars = 50 μm (*A–C*, *E–L*). *$P < 0.05$, *Sema3a*$^+$ gain-of-function vs. diabetic control mice.

detected MICAL1 in whole kidney lysates and in cultured podocytes (Fig. 7*A* and *B*). PlexinA$_1$, MICAL1, and β3 integrin were significantly downregulated in *Sema3a*$^+$ gain-of-function diabetic mice, whereas they were not dysregulated in control diabetic or nondiabetic mice (Fig. 7*A*), suggesting that changes in expression levels were caused by sema3a-induced severe diabetic nephropathy. Using coimmunoprecipitation, we determined that plexinA$_1$

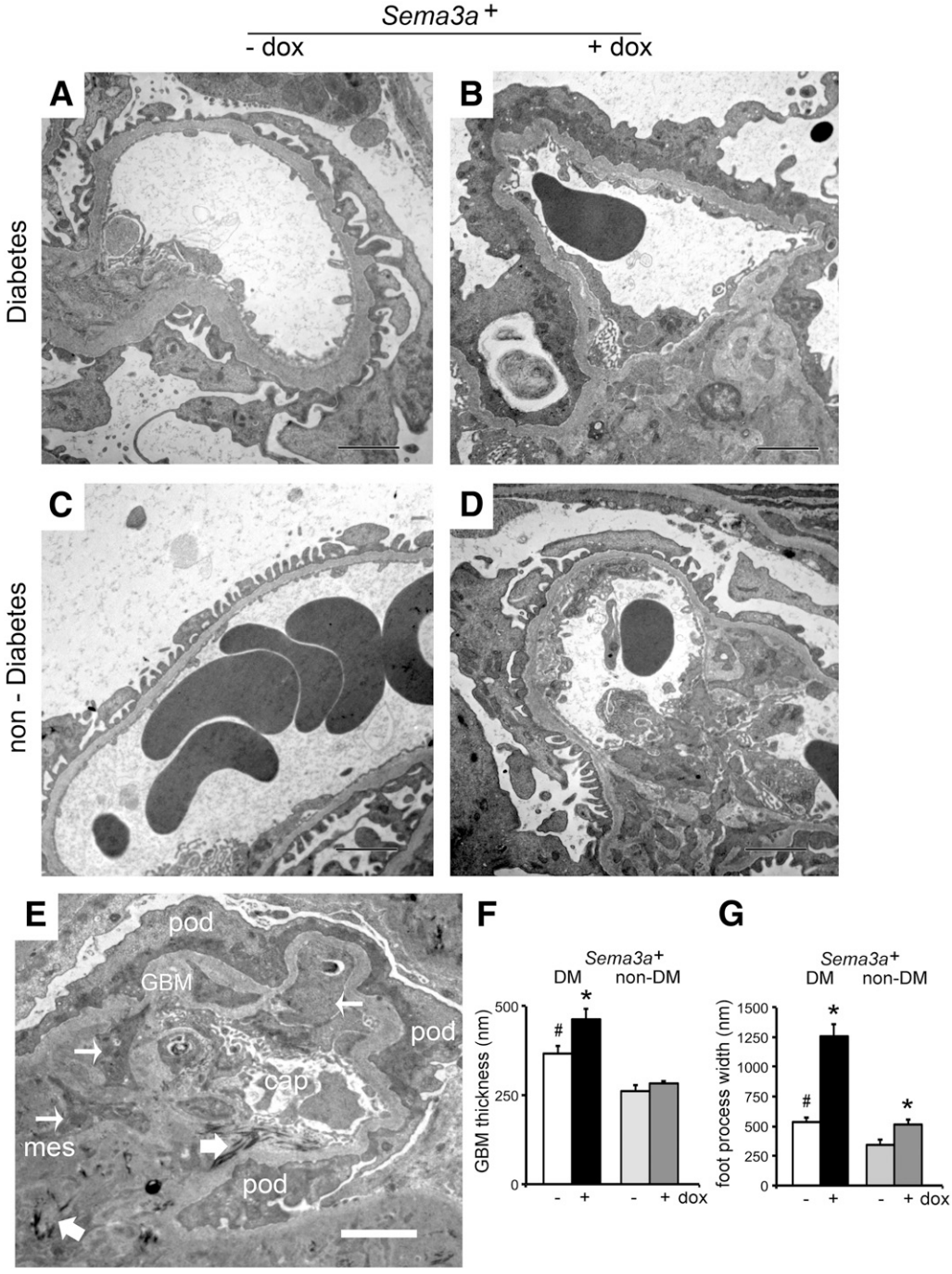

Figure 4—*Sema3a*$^+$ gain of function in diabetic mice causes diffuse foot process effacement (FPE), mesangial sclerosis, and endothelial injury. *A*: TEM shows focal FPE and a thick GBM in control diabetic glomeruli. *B*: TEM of *Sema3a*$^+$ gain-of-function diabetic glomeruli shows diffuse FPE, podocyte vacuolization, and absence of slit diaphragms, GBM thickening, mesangial sclerosis, and endothelial injury (endothelial cell swelling and expansion of the subendothelial space). *C*: TEM of nondiabetic control glomeruli show normal glomerular ultrastructure. *D*: TEM of nondiabetic *Sema3a*$^+$ gain-of-function glomeruli shows focal FPE, mild endothelial swelling, and mesangial sclerosis. *E*: *Sema3a*$^+$ gain-of-function diabetic glomerulus shows complete FPE with collapsed F-actin (darker gray), thick GBM, mesangial matrix (mes) interposition (thin arrows), extensive mesangial matrix accumulation with electron-dense fibrillar material (thick arrows), and narrow capillary lumen (cap). pod, podocyte. *F*: Quantitation of GBM thickness shows that excess sema3a exacerbates GBM thickening in diabetic mice (black bar vs. white bar), whereas it does not alter GBM in nondiabetic mice (gray bars). *G*: Quantitation of foot process width shows mild FPE in control mice with diabetes (DM) (white bar) and nondiabetics (non-DM) with excess sema3a (dark gray bar) and massive FPE (approximately threefold vs. control mice with diabetes) in *Sema3a*$^+$ gain-of-function mice with diabetes (black bar). Scale bars = 2 μm. dox, doxycycline.

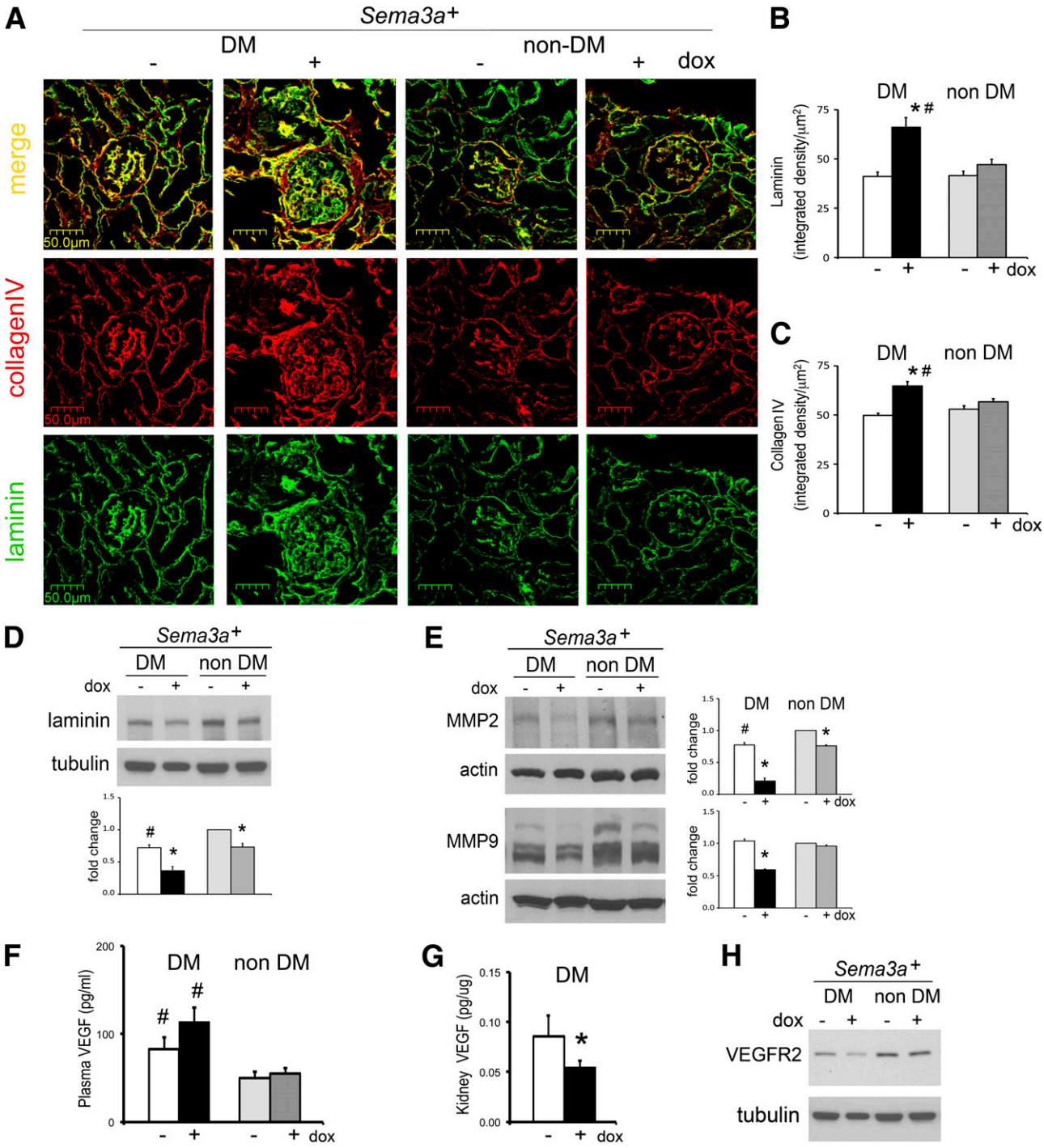

Figure 5—Laminin and collagen IV are increased in diabetic (DM)-Sema3a$^+$ glomerular nodules. *A*: Dual-fluorescent immunohistochemistry shows increased laminin (green) and collagen IV (red) colocalized to glomeruli from diabetic *Sema3a*$^+$ gain-of-function mice (DM-*Sema3a*$^+$ + doxycycline [dox]). Quantitation of immunoreactive laminin (*B*) and collagen IV (*C*) signals demonstrates a significant increase in glomeruli from diabetic *Sema3a*$^+$ gain-of-function mice. *D*: Western blotting shows decreased total kidney laminin in diabetic *Sema3a*$^+$gain-of-function kidneys. *E*: MMP-2 and -9 are downregulated in *Sema3a*$^+$ gain-of-function diabetic kidneys. *F–H*: Renal VEGF-A signaling is not upregulated in diabetic mice with *Sema3a*$^+$ gain of function. *F*: Plasma VEGF-A is elevated in all diabetic mice compared with nondiabetic mice, irrespective of *Sema3a*$^+$ gain-of-function induction. *G*: Kidney VEGF-A protein expression measured by ELISA is downregulated in diabetic mice with *Sema3a*$^+$ gain of function. *H*: VEGFR2 kidney protein expression is decreased in diabetic mice with *Sema3a*$^+$ gain of function. *$P < 0.05$ vs. corresponding control. #$P < 0.05$ vs. nondiabetic control.

interacts with MICAL1 in cultured podocytes (Fig. 7*C*). Moreover, actin coimmunoprecipitates with the plexinA_1–MICAL1 complex (Fig. 7*C*). To evaluate whether sema3a-induced podocyte F-actin collapse observed in vivo is caused by MICAL1-mediated actin depolymerization (21,22), we performed MICAL1 knockdown by siRNA in

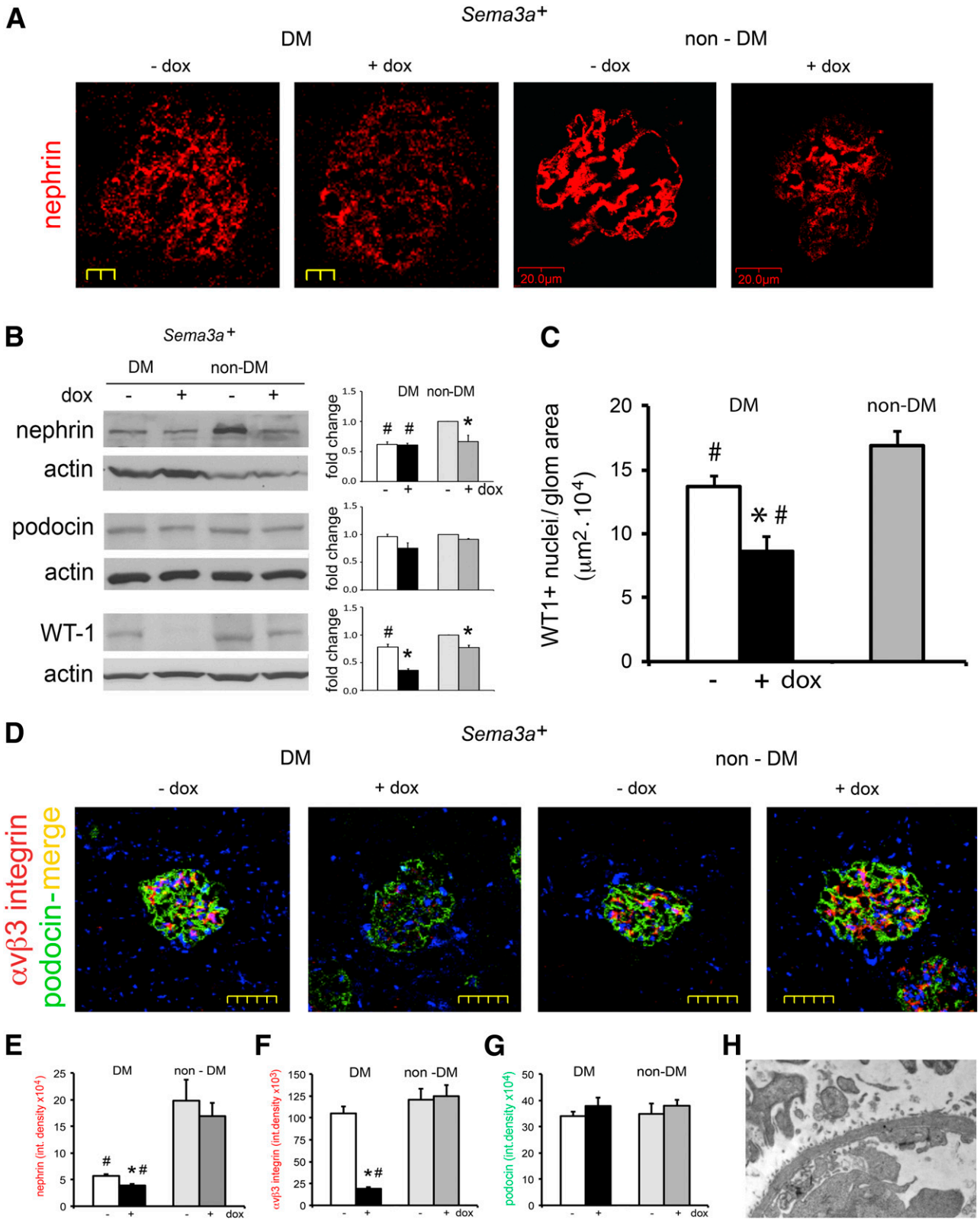

Figure 6—Combined nephrin, WT1, and αvβ3 integrin downregulation accentuates podocytopenia in diabetic *Sema3a*$^+$ gain-of-function mice. Nephrin downregulation is shown by immunofluorescence (IF) (*A*) and Western blotting (*B*) in all diabetic (DM) mice and in nondiabetic (non-DM) mice with excess sema3a; IF shows the least immunoreactive nephrin in *Sema3a*$^+$ gain-of-function diabetic glomeruli (*A* and *E*). Podocin immunoblotting and IF are not significantly changed by diabetic nephropathy or excess sema3a (*B* and *G*), except in severely damaged glomeruli (diabetic-*Sema3a*$^+$ + doxycycline [dox]; *D*). WT1 downregulation shown by immunoblotting (*B*) and IF WT1$^+$ podocyte counts (*C*) in diabetic *Sema3a*$^+$ gain-of-function kidneys (black bar), indicating podocytopenia; -dox and +dox nondiabetic WT1$^+$ podocyte counts were not different and were pooled (gray bar). *D*: Dual-IF shows αvβ3 integrin downregulation in diabetic *Sema3a*$^+$ gain-of-function

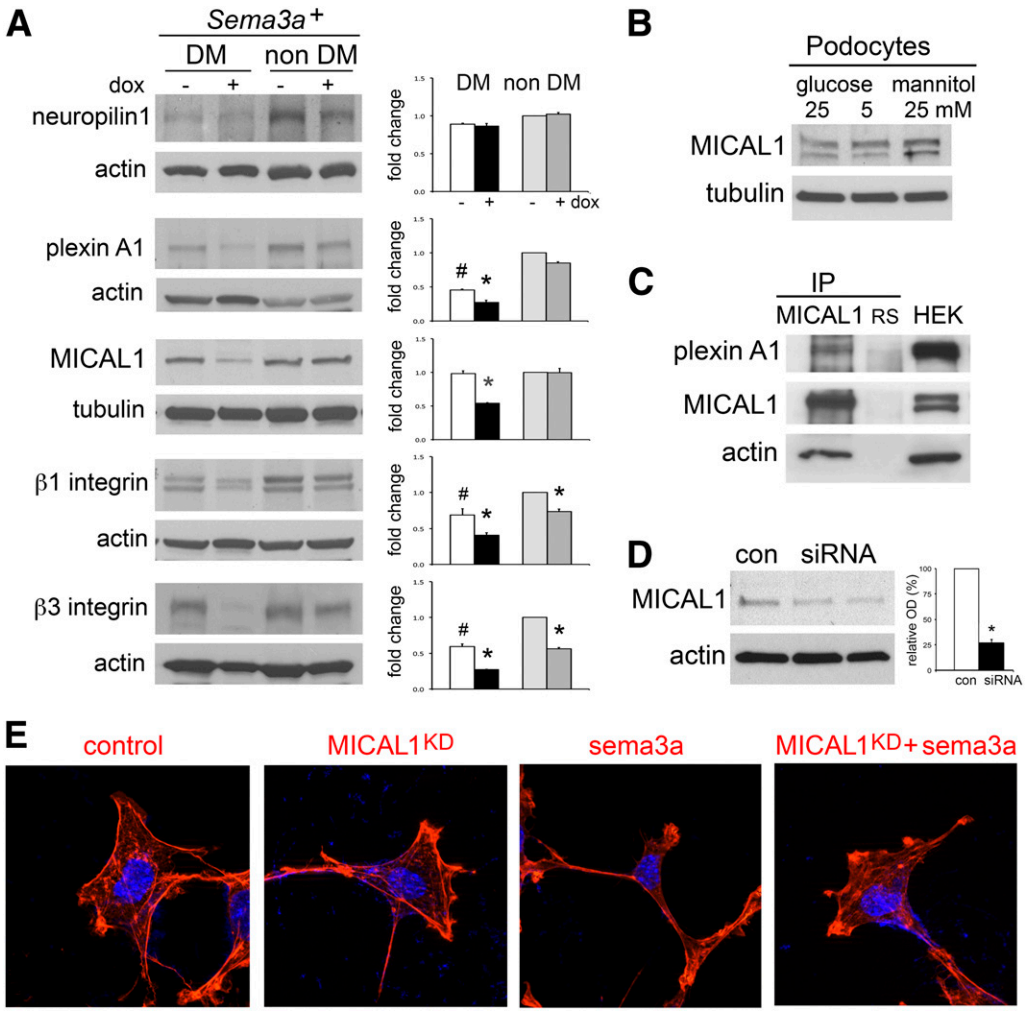

Figure 7—Sema3a signals in podocytes are mediated by MICAL1. *A*: Western blots show that the sema3a signaling pathway is expressed in the kidney. PlexinA$_1$, MICAL1, and β3 integrin are downregulated in *Sema3a*$^+$ gain-of-function diabetic (DM) mice (black bar). Quantitation by densitometry is shown in adjacent bar graphs. Data are expressed as mean ± SEM from three or more independent experiments. *B*: MICAL1 is expressed in cultured podocytes and is not altered by 4-h exposure to high glucose. *C*: Coimmunoprecipitation (IP) demonstrates an endogenous plexinA$_1$–MICAL1 interaction in podocytes; actin coprecipitates with the plexinA$_1$–MICAL1 complex. Rabbit serum (RS) and whole-cell lysate from HEK cells transiently transfected with full-length MICAL1 (HEK) were used as controls. *D*: Immunoblot shows MICAL1 knockdown of ~75% by siRNA, confirmed by densitometric analysis. *E*: MICAL1 knockdown (KD) prevents sema3a-induced podocyte contraction and F-actin collapse, assessed by rhodamine-phalloidin staining. Data from three or more independent experiments are shown. *P < 0.05 vs. corresponding control. #P < 0.05 vs. nondiabetic control. OD, optical density.

cultured podocytes, which decreased MICAL1 expression by 73 ± 2.6% (Fig. 7*D*). Using a cell assay and rhodamine-phalloidin staining (16), we determined that MICAL1 knockdown renders podocytes not susceptible to sema3a-induced contraction (Fig. 7*E*). Together, these findings indicate that MICAL1 mediates sema3a-induced podocyte F-actin collapse.

Xanthofulvin Prevents Sema3a-Induced Podocyte Damage and Attenuates Diabetic Nephropathy in Mice

Sema3a binding inhibitor xanthofulvin (30,31) prevented sema3a-induced podocyte F-actin collapse, shape change, and contraction (Fig. 8*A* and *B*), as assessed by rhodamine-phalloidin and morphometry. Next, we tested whether xanthofulvin infusion in vivo ameliorates the phenotype

glomeruli. Quantitation of glomerular IF signals for nephrin (*E*), αvβ3 integrin (*F*), and podocin (*G*). *H*: TEM from a *Sema3a*$^+$ gain-of-function diabetic glomerulus shows an open capillary loop with GBM "denuded" of podocytes, illustrating the severe podocytopenia assessed by low podocyte (WT1$^+$) counts shown in *C*. *P < 0.05 vs. corresponding control. #P < 0.05 vs. nondiabetic control. Scale bars = 20 μm (*A*), 50 μm (*D*), and 2 μm (*H*).

of *Sema3a*$^{+}$ gain-of-function diabetic mice. Xanthofulvin was administered by constant subcutaneous infusion (~1.8 μg/day) for 30 days (weeks 8–12), with no apparent side effect, stable body weight, and blood glucose (474 ± 28 mg/dL; Supplementary Fig. 2). Sema3a binding inhibition by xanthofulvin significantly decreases albuminuria, corrects hypoalbuminemia, abrogates renal insufficiency, and markedly attenuates the diabetic glomerulosclerosis phenotype of *Sema3a*$^{+}$ gain-of-function mice, as indicated by histology and TEM (Fig. 8*C–E*). Morphometric analysis revealed significantly decreased GBM thickness and foot process effacement in xanthofulvin-treated *Sema3a*$^{+}$ gain-of-function diabetic mice (Fig. 8*F*).

Deletion of *plexinA1* Attenuates Diabetic Nephropathy in Mice

We generated mice carrying a doxycycline-regulated, podocyte-specific *plexinA1* deletion (*plexinA1*^{pod}) to test

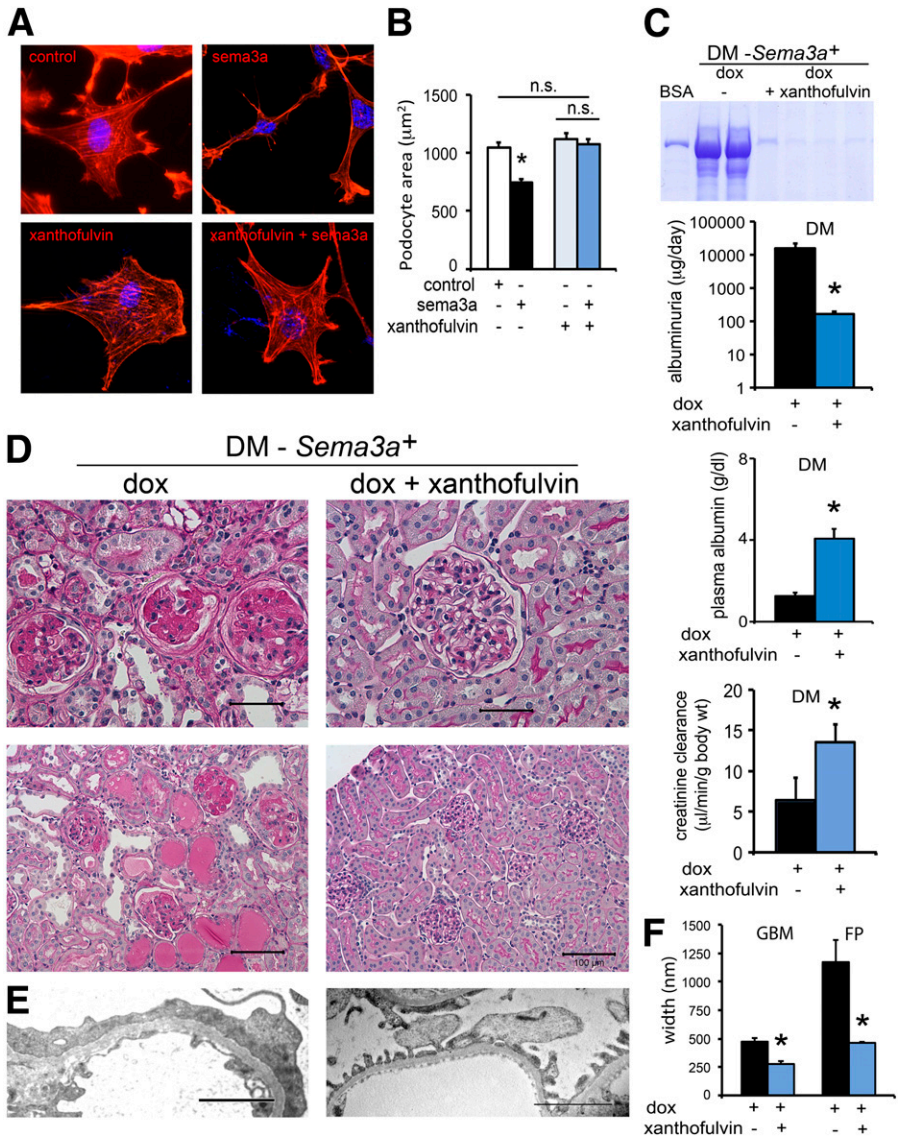

Figure 8—The sema3a inhibitor xanthofulvin ameliorated the sema3a-induced diabetic nephropathy phenotype in vivo and prevented podocyte contraction in vitro. Pretreatment with 0.1 μmol/L xanthofulvin for 60 min abrogates sema3a-induced podocyte F-actin collapse, shape change, and contraction as assessed by rhodamine-phalloidin staining (*A*) and cell area morphometric analysis (*B*). Scale bars = 20 μm. *C–E*: Constant subcutaneous infusion of xanthofulvin for 30 days (weeks 8–12 after diabetes onset) to *Sema3a*$^{+}$ gain-of-function diabetic (DM) mice (DM-*Sema3a*$^{+}$ + doxycycline [dox] + xanthofulvin) resulted in improved albuminuria, normalized plasma albumin and creatinine clearance (*C*, blue bars), mild mesangial hypercellularity, and extracellular matrix expansion (*D*, right panels) similar to control diabetic mice, a dramatic improvement from the diabetic nephropathy phenotype of *Sema3a*$^{+}$ gain-of-function diabetic mice (DM-*Sema3a*$^{+}$ +dox; left panels). Scale bars = 50 μm (top panels) and 100 μm (bottom panels). *E*: TEM: the left panel shows a thick GBM and complete foot process effacement (FPE) in *Sema3a*$^{+}$ gain-of-function diabetic glomerulus (+dox); the right panel shows focal FPE with a quite normal GBM in a glomerulus from a *Sema3a*$^{+}$ gain-of-function diabetic mouse receiving xanthofulvin infusion (+dox + xanthofulvin). Scale bars = 2 μm. *F*: Morphometry confirmed the improvement of GBM and foot process (FP) width (blue bars). Black bars are diabetic sema3a gain-of-function (+dox); blue bars are diabetic sema3a gain-of-function receiving xanthofulvin (+dox + xanthofulvin). *$P < 0.05$ vs. *Sema3a*$^{+}$ gain-of-function diabetic mice. n.s., not significant.

whether sema3a signaling in podocytes is responsible for the severe diabetic nephropathy phenotype observed in diabetic *Sema3a*$^+$ gain-of-function mice. In contrast to diabetic *Sema3a*$^+$ gain-of-function mice (Fig. 9*A*, *C*, and *E*), diabetic *Sema3a*$^+$*:plexinA1*^{pod} mice showed mild mesangial proliferation and only focal foot process effacement (Fig. 9*B*, *D*, *F*, and *I*), associated with mild albuminuria and normal creatinine clearance (Fig. 9*G* and *H*). *Sema3a*$^+$*:plexinA1*^{pod} and *Sema3a*$^+$ gain-of-function diabetic mice had similar hyperglycemia and severe polyuria (450 ± 26 vs. 533 ± 62 mg/dL, respectively; *P* = not significant; Supplementary Fig. 2). Collectively, *Sema3a*$^+$*:plexinA1*^{pod} mice revealed a diabetic nephropathy phenotype indistinguishable from that of diabetic *Sema3a*$^+$ gain-of-function mice treated with xanthofulvin or diabetic *Sema3a*$^+$ control mice, demonstrating that deletion of podocyte sema3a signaling attenuates diabetic nephropathy.

DISCUSSION

This study reveals that excess podocyte sema3a promotes the development of advanced diabetic nephropathy. We show that SEMA3A localized to glomerular podocytes is increased in advanced diabetic nephropathy in humans. We demonstrate that in diabetic mice, podocyte *Sema3a*$^+$ gain of function causes Kimmelstiel-Wilson-like nodular glomerulosclerosis, massive proteinuria, and renal insufficiency. We identify a signaling pathway that mediates sema3a-induced podocyte F-actin collapse by detecting plexinA_1 interaction with MICAL1 and actin in podocytes, demonstrating that MICAL1 is required to transduce sema3a effect to the podocyte actin cytoskeleton. We provide evidence that sema3a inhibition by xanthofulvin abrogates sema3a-induced podocyte contraction in vitro. Importantly, xanthofulvin-treatment or deletion of podocyte *plexinA1* abrogates

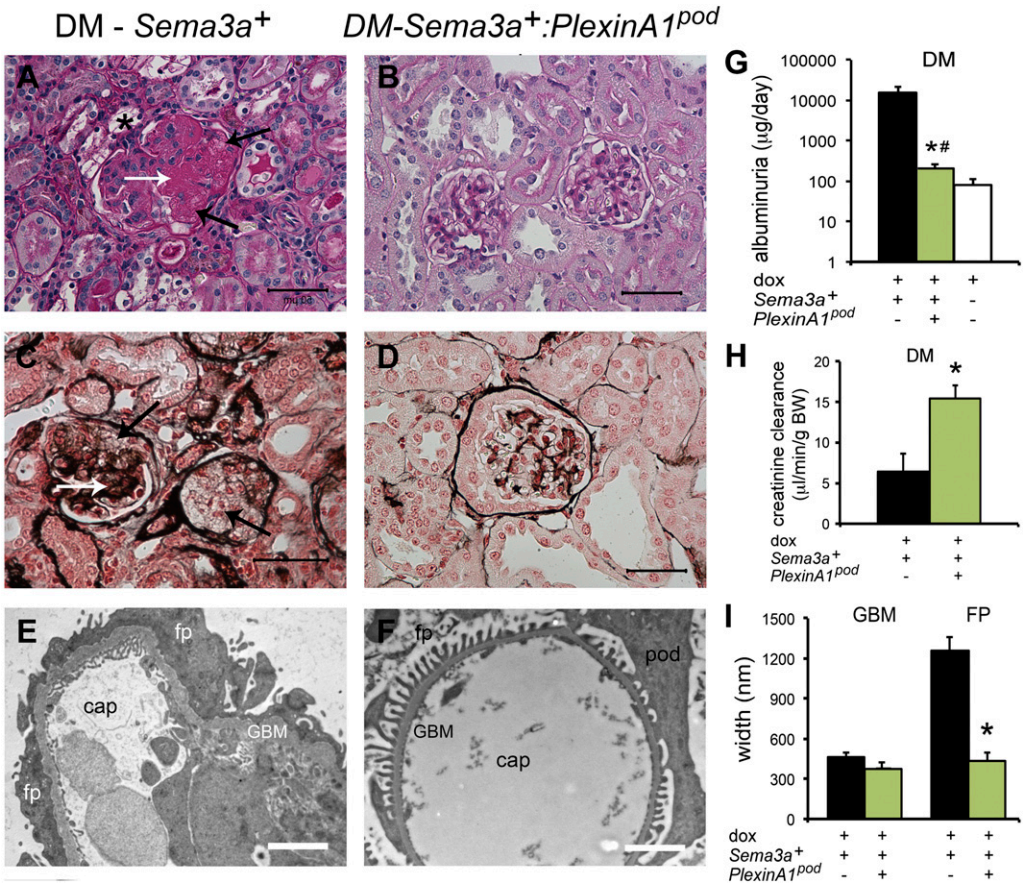

Figure 9—Deletion of podocyte *plexinA1* attenuates diabetic nephropathy in mice. *A–D*: Periodic acid Schiff and Jones' silver stains show severe diabetic (DM) nodular glomerulosclerosis in *Sema3a*$^+$ gain-of function kidneys (*A* and *C*) and mild mesangial expansion and otherwise normal histology in diabetic *Sema3a*$^+$*:plexinA1*^{pod} kidneys (*B* and *D*). *A*: *, foam cell; *A* and *C*: white arrows, nodule; black arrows, mesangiolysis. Scale bars = 50 µm. TEM shows complete foot process (FP) effacement, thickened GBM, and endothelial swelling in *Sema3a*$^+$ gain-of-function diabetic glomeruli (*E*), whereas TEM of *Sema3a*$^+$*:plexinA1*^{pod} mice shows very mild GBM thickening and virtually no FP effacement (*F*), as confirmed by morphometric analysis (*n* = 4 per group; *I*). Scale bars = 2 µm. *G* and *H*: Deletion of podocyte *plexinA1* in diabetic mice results in mild albuminuria and normal creatinine clearance (green bars), similar to that in wild-type diabetic mice (white bar), whereas *Sema3a*$^+$ gain of function causes massive albuminuria and renal insufficiency (black bars). Black bars are diabetic sema3a gain-of-function (+dox); green bars are diabetic plexinA1 knockout + sema3a gain-of-function (+dox); white bars are diabetic controls (-dox). *$P < 0.05$ vs. *Sema3a*$^+$ gain of function. #$P < 0.05$ vs. wild-type diabetic mice. BW, body weight; cap, capillary lumen; dox, doxycycline; pod, podocyte.

the diabetic nodular glomerulosclerosis resulting from *Sema3a*$^+$ gain of function in vivo.

Previous studies by our group and others established the essential roles of VEGF-A and nitric oxide in the pathogenesis of diabetic nephropathy (reviewed in refs. 6, 7, and 11). We previously observed sema3a upregulation in diabetic mice (24) and showed that podocyte-specific *Sema3a*$^+$ gain of function increases renal sema3a approximately threefold, leading to glomerular disease (15,16). Hence, we asked whether sema3a, which like VEGF-A is constitutively secreted by podocytes (14), plays a pathogenic role in diabetic nephropathy.

Here we demonstrate that podocyte SEMA3A is significantly increased in renal biopsies from patients with class III and IV diabetic nephropathy compared with nondiabetic patients with hypertension, obesity, or proteinuria caused by MCD. Although this finding does not elucidate the role of SEMA3A in diabetes, it suggests that dysregulation of semaphorin signaling might be relevant for human diabetic nephropathy. Increased tubular SEMA3A reported in renal biopsies from patients with lupus nephritis (32) was not observed in our study.

We found that podocyte *Sema3a*$^+$ gain of function in diabetic mice induces accelerated and advanced diabetic nephropathy, as defined by the AMDCC and the Renal Pathology Society criteria (33). Morphologically, diabetic mice with *Sema3a*$^+$ gain of function developed mesangiolysis and nodular glomerulosclerosis in >50% of glomeruli, extensive mesangial sclerosis, and interstitial fibrosis within 12–16 weeks. Moreover, *Sema3a*$^+$ gain-of-function glomerular histology and TEM revealed multiple features of human advanced diabetic nephropathy (34), including diffuse GBM thickening, widespread effacement and fusion of podocyte foot processes, marked podocytopenia, Kimmelstiel-Wilson-like nodular lesions, endothelial injury, fibrin caps, and vascular pole hyalinosis. Few mouse models of diabetic nephropathy have developed diabetic nodular glomerulosclerosis, namely *eNOS* knockout (35,36), β-cell calmodulin transgenics (37,38), podocyte-*VEGF-A* gain-of-function (24), and BTBR *Ob/Ob* mice (39). In most of these models, nodules become apparent late in the course of the disease (≥5 months), except podocyte-*VEGF-A* gain of function (24). Genetic background might contribute to these time frame differences; FVB mice are thought to be more susceptible to diabetic nephropathy than B6 mice (40). Although *Sema3a*$^+$ gain of function resulted in endothelial injury in both diabetic and nondiabetic kidneys, fibrin or other evidence of thrombotic microangiopathy was not observed, suggesting that the phenotype was caused by severe diabetic nephropathy rather than an overlap of diabetes and nondiabetic renal disease, as described in humans (41). Genetic manipulation of *Nos3*, *Vegf-a*, *Bkr1–2*, and obesity in the setting of diabetes resulted in the most informative mouse models of advanced diabetic nephropathy (35,36,39,42), consistent with *NOS3* and *VEGF-A* polymorphisms linked to human diabetic nephropathy (6,43). Similarly, *Sema3a*$^+$ gain-of-function diabetic mice develop the most advanced nodular glomerulosclerosis reported so far, mimicking class IV human diabetic nephropathy.

Functionally, *Sema3a*$^+$ gain-of-function diabetic mice developed massive proteinuria, leading to hypoalbuminemia and renal insufficiency, suggesting progressive diabetic nephropathy, consistent with the advanced morphologic phenotype. Previous mouse models of diabetic nodular glomerulosclerosis have shown some, but not all, of these functional abnormalities at once. For example, diabetic *eNOS* knockout mice doubled their baseline blood urea nitrogen and increased albuminuria approximately fourfold 5 months after the disease onset (36); β-cell calmodulin transgenic mice developed hyperfiltration, massive proteinuria, and hypoalbuminemia at ≥6 months (37,38), and podocyte-*VEGF-A* gain-of-function mice showed massive proteinuria and decreased hyperfiltration 3 months after disease onset (24), whereas *BTBR Ob/Ob* mice developed hyperfiltration and massive albuminuria at 5 months of age (39).

Normal circulating sema3a concentrations in mice and humans are not well established. We found that diabetes per se does not increase plasma concentrations of sema3a in mice; sema3a was similar in control diabetic and nondiabetic mice. By contrast, podocyte *Sema3a*$^+$ gain of function increases plasma concentrations of sema3a, and severe diabetic nephropathy seems to have an additive effect, probably because of decreased glomerular filtration rate, as suggested by an inverse correlation of plasma sema3a concentration with creatinine clearance in diabetic mice. Interestingly, the range of increase in plasma sema3a concentration (approximately threefold) is similar to that of VEGF-A reported in diabetic mice and humans (24,44). Myocardial-specific sema3a transgenic mice develop ventricular tachyarrhythmia and sudden death (25); unfortunately, their plasma concentrations of sema3a were not reported. Further studies will elucidate whether circulating sema3a concentration could be used as a biomarker of diabetic nephropathy, cardiovascular risk, and/or disease progression.

Plasma VEGF-A is elevated in STZ-induced diabetes, irrespective of *Sema3a* transgene induction. Since local VEGF-A signaling at the glomerular filtration barrier, rather than a higher circulating concentration, mediated advanced diabetic nephropathy (24), we measured kidney VEGF-A and VEGFR2, which were downregulated in *Sema3a*$^+$ gain-of-function diabetic mice, indicating decreased VEGF-A signaling. Podocytopenia and sema3a competition with VEGF-A for neuropilin1 binding, abrogating local amplification of VEGFR2 signaling, likely underlie these observations (19). Together, these findings argue that the advanced diabetic nephropathy phenotype observed in *Sema3a*$^+$ gain-of-function diabetic mice is not attributable to excess VEGF-A signaling.

Elegant studies have elucidated sema3a effects on multiple cell types and signaling pathways conserved

from flies to humans (reviewed in refs. 12 and 13). Sema3a repulsive cues lead to cell contraction (or retraction) by regulating actin dynamics (16,22,23,45). Landmark studies showed that sema3a decreases motility and induces F-actin collapse in endothelial cells (19,45). We demonstrated that both sema3a receptors are expressed in podocytes, transducing cell-autonomous sema3a signals that induce podocyte contraction and apoptosis in vitro and in vivo (14–16,46). Additional studies demonstrated that plexinA_1 interacts directly with nephrin (16). Here, we identify for the first time MICAL1 protein in the kidney and in cultured podocytes. We also demonstrate that plexinA_1, MICAL1, and actin interact in podocytes. Upon sema3a binding to the neuropilin–plexinA_1 complex, a direct interaction between the MICAL1 C-terminus and the plexinA_1 cytoplasmic domain releases MICAL1 autoinhibition and is required for sema3a signaling (20,47). MICAL1 is a mono-oxygenase flavoprotein that selectively oxidizes actin Met46 and Met49 residues to disassemble F-actin in a reversible, redox-dependent manner (22,23,46). MICAL1 knockdown in cultured podocytes revealed that MICAL1 is required for sema3a-induced podocyte shape changes and F-actin collapse and suggests that sema3a signaling may lead to H_2O_2 generation by MICAL1 in podocytes. This mechanism might be a critical contributor to sema3a-induced podocyte and endothelial injury. The important role of reactive oxygen species in diabetic nephropathy is well established, although the beneficial effect of antioxidants on diabetic nephropathy is considered limited (reviewed in refs. 2, 3, and 6). Identifying and targeting specific mechanisms generating reactive oxygen species, such as MICAL1, may unravel a novel therapeutic approach to diabetic nephropathy.

A key finding of this study is that xanthofulvin abrogates sema3a-induced podocyte F-actin collapse in vitro and attenuates diabetic nephropathy in mice. Xanthofulvin is a specific sema3a competitive binding inhibitor, naturally produced by penicillium SPF-3059 and purified (28) or synthesized de novo (31). Both fungal and synthetic xanthofulvin prevent sema3a-induced growth cone collapse in vitro (31,48). Moreover, purified fungal xanthofulvin promotes functional recovery of injured spinal cord by decreasing apoptosis and enhancing angiogenesis in vivo (49). Because of the limited availability of fungal xanthofulvin, we performed in vitro experiments using synthetic xanthofulvin. We determined that sema3a inhibition by xanthofulvin has no deleterious effects on cultured podocytes. Most notably, xanthofulvin infusion administered in vivo to diabetic *Sema3a*$^+$ gain-of-function mice decreased albuminuria and abrogated renal insufficiency and the diabetic nodular glomerulosclerosis phenotype, providing proof of principle that targeting sema3a is beneficial in diabetic nephropathy.

To further confirm the relevant pathogenic role of increased sema3a signaling in diabetic nephropathy, we deleted podocyte *plexinA1* in *Sema3a*$^+$ diabetic mice to abrogate sema3a signaling. Notably, diabetic *plexinA1* ^{pod}: *Sema3a*$^+$ mice developed a mild diabetic nephropathy phenotype remarkably similar to that of xanthofulvin-treated and uninduced *Sema3a*$^+$ diabetic mice. Together, these findings demonstrate that excess sema3a signaling exacerbates diabetic nephropathy in mice.

Additional studies using other severe genetic type 1 and type 2 diabetic nephropathy models are needed to establish whether inhibiting sema3a signaling can prevent diabetic nephropathy or stop progression. Collectively, our findings in human advanced diabetic nephropathy renal biopsies and mechanistic studies of diabetic mice suggest that establishing SEMA3A concentrations in healthy and diabetic individuals and their correlation with estimated glomerular filtration rate, proteinuria, and glomerular immunoreactive SEMA3A in renal biopsies would advance our understanding of diabetic nephropathy. Sema3a is thought to function as an osteoprotective factor, a negative regulator of immune response and angiogenesis, an arrhythmogenic factor, and a potential biomarker of acute kidney injury (25,50–52). Future studies targeting the sema3a signaling pathway should also evaluate these functions. This study identifies podocyte SEMA3A upregulation in biopsies from humans with advanced diabetic nephropathy. Excess sema3a plays a pathogenic role in diabetic nephropathy in mice, leading to severe diabetic nodular glomerulosclerosis, massive proteinuria, and renal failure, which can be attenuated by a sema3a inhibitor or *plexinA1* deletion. MICAL1 mediates sema3a–plexinA_1 signals in podocytes, leading to F-actin collapse. Collectively, these findings indicate that excess sema3a promotes severe diabetic nephropathy and identifies novel potential therapeutic targets.

Acknowledgments. The authors thank Valerie Castellani (Centre de Génétique et de Physiologie Moléculaire et Cellulaire, Lyon, France) and Stephen Strittmatter (Yale School of Medicine) for providing plexinA_1 and MICAL1 constructs, Toru Kimura and Kaoru Kikuchi (Dainippon Sumitomo Pharma Co.) for providing fungal xanthofulvin, Sestan Nenad (Yale School of Medicine) for providing *plexinA1*$^{f/f}$ mice, Jeroen Pasterkamp (Brain Center Rudolf Magnus University Medical Center, Utrecht, the Netherlands) for providing mMical1 siRNA sequence, Tong Wang (Yale School of Medicine) for implanting Alzet pumps, and Lonette Diggs (Yale School of Medicine) for albumin ELISA measurements.

Funding. This work was funded by National Institutes of Health grant R01-DK-064187, DK-098824 (to A.T.), and P30-DK-079310 (George M. O'Brien Kidney Center at Yale).

Duality of Interest. No potential conflicts of interest relevant to this article were reported.

Author Contributions. P.K.A. and D.V. performed experiments and analyzed data. D.B.T., D.S., G.M., and M.K. contributed human samples and reagents and analyzed data. A.T. designed the experiments, analyzed data, and wrote the manuscript. A.T. is the guarantor of this work and, as such, had full access to all the data in the study and takes responsibility for the integrity of the data and the accuracy of the data analysis.

References

1. Fineberg D, Jandeleit-Dahm KA, Cooper ME. Diabetic nephropathy: diagnosis and treatment. Nat Rev Endocrinol 2013;9:713–723

2. Forbes JM, Cooper ME. Mechanisms of diabetic complications. Physiol Rev 2013;93:137–188
3. Badal SS, Danesh FR. New insights into molecular mechanisms of diabetic kidney disease. Am J Kidney Dis 2014;63(Suppl 2):S63–S83
4. Breyer MD. Drug discovery for diabetic nephropathy: trying the leap from mouse to man. Semin Nephrol 2012;32:445–451
5. Mogensen CE, Christensen CK, Vittinghus E. The stages in diabetic renal disease. With emphasis on the stage of incipient diabetic nephropathy. Diabetes 1983;32(Suppl. 2):64–78
6. Tufro A, Veron D. VEGF and podocytes in diabetic nephropathy. Semin Nephrol 2012;32:385–393
7. Gnudi L. Cellular and molecular mechanisms of diabetic glomerulopathy. Nephrol Dial Transplant 2012;27:2642–2649
8. Dessapt-Baradez C, Woolf AS, White KE, et al. Targeted glomerular angiopoietin-1 therapy for early diabetic kidney disease. J Am Soc Nephrol 2014; 25:33–42
9. Suzuki H, Usui I, Kato I, et al. Deletion of platelet-derived growth factor receptor-β improves diabetic nephropathy in Ca^{2+}/calmodulin-dependent protein kinase IIα (Thr286Asp) transgenic mice. Diabetologia 2011;54:2953–2962
10. Sung SH, Ziyadeh FN, Wang A, Pyagay PE, Kanwar YS, Chen S. Blockade of vascular endothelial growth factor signaling ameliorates diabetic albuminuria in mice. J Am Soc Nephrol 2006;17:3093–3104
11. Nakagawa T, Kosugi T, Haneda M, Rivard CJ, Long DA. Abnormal angiogenesis in diabetic nephropathy. Diabetes 2009;58:1471–1478
12. Tran TS, Kolodkin AL, Bharadwaj R. Semaphorin regulation of cellular morphology. Annu Rev Cell Dev Biol 2007;23:263–292
13. Hung RJ, Terman JR. Extracellular inhibitors, repellents, and semaphorin/plexin/MICAL-mediated actin filament disassembly. Cytoskeleton (Hoboken) 2011;68:415–433
14. Villegas G, Tufro A. Ontogeny of semaphorins 3A and 3F and their receptors neuropilins 1 and 2 in the kidney. Mech Dev 2002;119(Suppl. 1):S149–S153
15. Reidy KJ, Villegas G, Teichman J, et al. Semaphorin3a regulates endothelial cell number and podocyte differentiation during glomerular development. Development 2009;136:3979–3989
16. Reidy KJ, Aggarwal PK, Jimenez JJ, Thomas DB, Veron D, Tufro A. Excess podocyte semaphorin-3A leads to glomerular disease involving plexinA1-nephrin interaction. Am J Pathol 2013;183:1156–1168
17. Kolodkin AL, Levengood DV, Rowe EG, Tai YT, Giger RJ, Ginty DD. Neuropilin is a semaphorin III receptor. Cell 1997;90:753–762
18. Takahashi T, Fournier A, Nakamura F, et al. Plexin-neuropilin-1 complexes form functional semaphorin-3A receptors. Cell 1999;99:59–69
19. Miao HQ, Soker S, Feiner L, Alonso JL, Raper JA, Klagsbrun M. Neuropilin-1 mediates collapsin-1/semaphorin III inhibition of endothelial cell motility: functional competition of collapsin-1 and vascular endothelial growth factor-165. J Cell Biol 1999;146:233–242
20. Terman JR, Mao T, Pasterkamp RJ, Yu HH, Kolodkin AL. MICALs, a family of conserved flavoprotein oxidoreductases, function in plexin-mediated axonal repulsion. Cell 2002;109:887–900
21. Hung RJ, Yazdani U, Yoon J, et al. Mical links semaphorins to F-actin disassembly. Nature 2010;463:823–827
22. Hung RJ, Pak CW, Terman JR. Direct redox regulation of F-actin assembly and disassembly by Mical. Science 2011;334:1710–1713
23. Hung RJ, Spaeth CS, Yesilyurt HG, Terman JR. SelR reverses Mical-mediated oxidation of actin to regulate F-actin dynamics. Nat Cell Biol 2013;15:1445–1454
24. Veron D, Bertuccio CA, Marlier A, et al. Podocyte vascular endothelial growth factor ($Vegf_{164}$) overexpression causes severe nodular glomerulosclerosis in a mouse model of type 1 diabetes. Diabetologia 2011;54:1227–1241
25. Ieda M, Kanazawa H, Kimura K, et al. Sema3a maintains normal heart rhythm through sympathetic innervation patterning. Nat Med 2007;13:604–612
26. Perl AK, Wert SE, Nagy A, Lobe CG, Whitsett JA. Early restriction of peripheral and proximal cell lineages during formation of the lung. Proc Natl Acad Sci U S A 2002;99:10482–10487
27. Takegahara N, Takamatsu H, Toyofuku T, et al. Plexin-A1 and its interaction with DAP12 in immune responses and bone homeostasis. Nat Cell Biol 2006;8: 615–622
28. Veron D, Aggarwal PK, Velazquez H, Kashgarian M, Moeckel G, Tufro A. Podocyte-specific VEGF-a gain of function induces nodular glomerulosclerosis in eNOS null mice. J Am Soc Nephrol 2014;25:1814–1824
29. Zhou Y, Adolfs Y, Pijnappel WW, et al. MICAL-1 is a negative regulator of MST-NDR kinase signaling and apoptosis. Mol Cell Biol 2011;31:3603–3615
30. Kumagai K, Hosotani N, Kikuchi K, Kimura T, Saji I. Xanthofulvin, a novel semaphorin inhibitor produced by a strain of Penicillium. J Antibiot (Tokyo) 2003; 56:610–616
31. Axelrod A, Eliasen AM, Chin MR, Zlotkowski K, Siegel D. Syntheses of xanthofulvin and vinaxanthone, natural products enabling spinal cord regeneration. Angew Chem Int Ed Engl 2013;52:3421–3424
32. Vadasz Z, Haj T, Halasz K, et al. Semaphorin 3A is a marker for disease activity and a potential immunoregulator in systemic lupus erythematosus. Arthritis Res Ther 2012;14:R146
33. Tervaert TW, Mooyaart AL, Amann K, et al.; Renal Pathology Society. Pathologic classification of diabetic nephropathy. J Am Soc Nephrol 2010;21: 556–563
34. Nishi S, Ueno M, Hisaki S, et al. Ultrastructural characteristics of diabetic nephropathy. Med Electron Microsc 2000;33:65–73
35. Zhao HJ, Wang S, Cheng H, et al. Endothelial nitric oxide synthase deficiency produces accelerated nephropathy in diabetic mice. J Am Soc Nephrol 2006;17:2664–2669
36. Nakagawa T, Sato W, Glushakova O, et al. Diabetic endothelial nitric oxide synthase knockout mice develop advanced diabetic nephropathy. J Am Soc Nephrol 2007;18:539–550
37. Yuzawa Y, Niki I, Kosugi T, et al. Overexpression of calmodulin in pancreatic beta cells induces diabetic nephropathy. J Am Soc Nephrol 2008;19: 1701–1711
38. Zheng S, Noonan WT, Metreveli NS, et al. Development of late-stage diabetic nephropathy in OVE26 diabetic mice. Diabetes 2004;53:3248–3257
39. Hudkins KL, Pichaiwong W, Wietecha T, et al. BTBR Ob/Ob mutant mice model progressive diabetic nephropathy. J Am Soc Nephrol 2010;21:1533–1542
40. Brosius FC 3rd, Alpers CE, Bottinger EP, et al.; Animal Models of Diabetic Complications Consortium. Mouse models of diabetic nephropathy. J Am Soc Nephrol 2009;20:2503–2512
41. Sharma SG, Bomback AS, Radhakrishnan J, et al. The modern spectrum of renal biopsy findings in patients with diabetes. Clin J Am Soc Nephrol 2013;8: 1718–1724
42. Kakoki M, Sullivan KA, Backus C, et al. Lack of both bradykinin B1 and B2 receptors enhances nephropathy, neuropathy, and bone mineral loss in Akita diabetic mice. Proc Natl Acad Sci U S A 2010;107:10190–10195
43. Ezzidi I, Mtiraoui N, Mohamed MB, Mahjoub T, Kacem M, Almawi WY. Association of endothelial nitric oxide synthase Glu298Asp, 4b/a, and -786T>C gene variants with diabetic nephropathy. J Diabetes Complications 2008;22: 331–338
44. Hovind P, Tarnow L, Oestergaard PB, Parving HH. Elevated vascular endothelial growth factor in type 1 diabetic patients with diabetic nephropathy. Kidney Int Suppl 2000;75:S56–S61
45. Serini G, Valdembri D, Zanivan S, et al. Class 3 semaphorins control vascular morphogenesis by inhibiting integrin function. Nature 2003;424:391–397
46. Guan F, Villegas G, Teichman J, Mundel P, Tufro A. Autocrine class 3 semaphorin system regulates slit diaphragm proteins and podocyte survival. Kidney Int 2006;69:1564–1569

47. Schmidt EF, Shim SO, Strittmatter SM. Release of MICAL autoinhibition by semaphorin-plexin signaling promotes interaction with collapsin response mediator protein. J Neurosci 2008;28:2287–2297
48. Kikuchi K, Kishino A, Konishi O, et al. In vitro and in vivo characterization of a novel semaphorin 3A inhibitor, SM-216289 or xanthofulvin. J Biol Chem 2003; 278:42985–42991
49. Lee BC, Péterfi Z, Hoffmann FW, et al. MsrB1 and MICALs regulate actin assembly and macrophage function via reversible stereoselective methionine oxidation. Mol Cell 2013;51:397–404
50. Kaneko S, Iwanami A, Nakamura M, et al. A selective Sema3A inhibitor enhances regenerative responses and functional recovery of the injured spinal cord. Nat Med 2006;12:1380–1389
51. Hayashi M, Nakashima T, Taniguchi M, Kodama T, Kumanogoh A, Takayanagi H. Osteoprotection by semaphorin 3A. Nature 2012;485:69–74
52. Jayakumar C, Ranganathan P, Devarajan P, Krawczeski CD, Looney S, Ramesh G. Semaphorin 3A is a new early diagnostic biomarker of experimental and pediatric acute kidney injury. PLoS One 2013;8:e58446